

Generation and Characterization of Monoclonal Antibodies to NIAM: A Nuclear Interactor of ARF and Mdm2

Jussara Hagen,¹ Van Tompkins,¹ Amel Dudakovic,¹ Jamie A. Weydert,² and Dawn E. Quelle^{1,3}

Abstract

Nuclear interactor of ARF and Mdm2 (NIAM) is a newly discovered growth inhibitor that helps maintain chromosomal stability. It is functionally linked to the ARF-Mdm2-p53 tumor suppressor pathway and is predicted to be a tumor suppressor, but the lack of antibodies capable of detecting the endogenous human protein has delayed efforts to define its role in human tumorigenesis. This study reports the development, screening, and characterization of several monoclonal antibodies (MAbs) that specifically recognize endogenous human NIAM protein by Western blotting, immunoprecipitation, immunofluorescence, and immunohistochemistry. These MAbs are predicted to be important tools for evaluating the expression and physiological function of NIAM in normal versus neoplastic human cells and tissues.

Introduction

CANCER ARISES FROM VARIOUS GENETIC ALTERATIONS that disable cell cycle checkpoints and enable cells to survive and proliferate in the face of genotoxic insults, such as DNA damage.⁽¹⁾ One of the most important checkpoint regulators is p53, a transcription factor whose activation by numerous cellular stresses causes permanent cell cycle arrest or apoptosis.⁽²⁾ Loss of p53 function, both through mutation or deletion of the p53 gene or deregulation of its many activators and inhibitors, removes those protective brakes to the cell cycle and is a defining feature of nearly all human cancers.⁽³⁾ Indeed, genetic inactivation of p53 occurs in over 50% of human tumors⁽⁴⁾ while loss of its key activator, the alternative reading frame (ARF) tumor suppressor,⁽⁵⁾ is the second most common event during carcinogenesis.⁽⁶⁾ Most human cancers also overexpress the p53 antagonist Mdm2, which likewise results in p53 inactivation.⁽⁷⁻⁹⁾

ARF stimulates p53 in response to aberrant oncogenic signaling and is essential for maintaining its activity following DNA damage.^(7,10) Most evidence suggests that ARF primarily functions by binding and inhibiting Mdm2, an E3 ubiquitin ligase that targets p53 for degradation.⁽⁸⁾ However, ARF has many known binding partners and can prevent cancer independent of p53 through antiprolifera-

tive pathways that are only partly defined.^(8,11) We recently discovered several new binding partners of ARF that contribute to both its p53-dependent and p53-independent signaling pathways^(12,13) (also, unpublished data, V. Tompkins and D.E. Quelle). One of those partners is a novel protein we named *NIAM* because it was found to be a nuclear interactor of ARF and Mdm2.⁽¹³⁾ NIAM is normally expressed at low levels in cells due to Mdm2-mediated ubiquitination and degradation. When overexpressed, NIAM inhibits cell cycle progression, enhances ARF stability, and activates p53. NIAM also has undefined ARF- and p53-independent activities that help it maintain chromosomal stability.

Little else is currently known about the normal function and regulation of NIAM during tumorigenesis, although the above data strongly suggest NIAM may be a tumor suppressor protein. A major impediment to studying NIAM's role in cancer, however, has been the inability of existing NIAM polyclonal antibodies to detect endogenous NIAM protein expression in normal and transformed human cells. Therefore, we began the development and characterization of monoclonal antibodies (MAbs) to human NIAM. Here we describe the identification of several MAbs that effectively recognize endogenous human NIAM protein using multiple molecular approaches.

¹Department of Pharmacology, ²Department of Pathology, ³Molecular and Cellular Biology Graduate Program, The University of Iowa, College of Medicine, Iowa City, Iowa.

Materials and Methods

Bacterial protein expression and purification

Wild-type human NIAM (hNIAM) cDNA was subcloned into the pGEX-2T vector and expressed as a glutathione S-transferase (GST) fusion protein in BL21 *E. coli* following induction with IPTG (1 mM) for 3 h at 37°C. Soluble GST-hNIAM protein was recovered from bacterial cell lysates on glutathione S-Sepharose (Amersham Biosciences, Piscataway, NJ), washed three times in NETN lysis buffer (120 mM NaCl, 1 mM EDTA, 50 mM Tris-HCl [pH 8.0], 0.5% NP-40), and eluted with 20 mM glutathione in elution buffer (50 mM Tris-HCl, 150 mM NaCl, 0.1 mM EDTA, 5 mM DTT [pH 8.0]). GST-hNIAM was then dialysed into phosphate-buffered saline (PBS) and concentrated to approximately 1 mg/mL using centricon-30 filtration units (Millipore, Bedford, MA), as described by the manufacturer. Purified GST-hNIAM was quantified by BCA assay (Pierce Biotechnology, Rockford, IL) and used as antigen to immunize mice. Untagged hNIAM protein was then recovered from the remaining Sepharose-bound GST-hNIAM pool by cleavage with thrombin (Amersham Biosciences) and separated from GST by SDS-PAGE, and the band containing the protein was sliced out of an unfixed Coomassie-stained gel (0.05% Coomassie blue in ddH₂O for 5 min). The protein was extracted from the gel by overnight incubation at 30°C in 2.5% 2-mercaptoethanol, 1% SDS, and 50 mM Tris-HCl [pH 6.8]. The majority of SDS was removed by precipitation at 4°C and the sample was concentrated and dialysed into PBS as described above. The hNIAM protein was quantified and used for screening the monoclonal antibodies.

Immunization of mice and generation of hybridomas

Two female Balb/c mice (National Cancer Institute, Frederick, MD) were immunized with three rounds of injections per animal using 100 µg GST-hNIAM protein in TiterMax (Sigma-Aldrich, St. Louis, MO) adjuvant per injection. Two booster immunizations were given at 2 week intervals, and test bleeds were assayed for their ability to recognize recombinant hNIAM protein by Western blotting.

Once positive bleeds were obtained, cell fusions were generated after one additional boost. The mouse with the more positive test bleed was euthanized and its spleen removed under aseptic conditions into a Petri dish containing 5 mL of HEPES buffered RPMI 1640 with 10% activated fetal calf serum (C-TCM). A single cell suspension of splenocytes was prepared by gently teasing apart the spleen, and cells were pelleted and resuspended in 5 mL C-TCM (~4 × 10⁷ c/mL). Logarithmically growing NSI myeloma cells were also pelleted and resuspended in 5 mL C-TCM at roughly 4 × 10⁶ c/mL. Splenocytes and myeloma cells were mixed at a 10:1 ratio (splenocytes–myeloma cells), incubated at 37°C for 5 min, and centrifuged at 1000 rpm for 5 min. The supernatant was aspirated, the tube tapped gently to loosen the cell pellet, and 1.5 mL of 50% PEG 1400 (Aldrich Chemical Company, Milwaukee, WI) added over a 1 min period while keeping the tube at 37°C. The mixture was incubated one additional minute with gentle mixing, and 10 mL HEPES buffered 1640 RPMI (no fcs) was added slowly over a 3 min period. Cells were then centrifuged as above, resuspended in 200 mL C-TCM containing 1 × 10⁻⁴ M hypoxanthine, 4 ×

10⁻⁷ M aminopterin, and 1.6 × 10⁻⁵ M thymidine, distributed into ten 96-well plates (200 µL per well), and incubated for 10 days at 37°C prior to primary screening.

Monoclonal antibody screening

Monoclonal antibody (MAb) supernatants were screened using a 96-well Bio-Dot Microfiltration apparatus (Bio-Rad, Hercules, CA), according to the manufacturer's instructions. Briefly, purified hNIAM (15 ng/well) was bound to nitrocellulose and the membrane incubated with blocking solution (3% BSA in Tris-buffered saline containing 0.1% Tween-20 [TBST]) via gravity flow. MAb supernatants (10 µL per well) were pooled together into a 96-well plate using a multi-well pipettor such that all 12 wells from a single row of each 96-well plate were combined. Consequently 80 pools containing 12 different MAb supernatants (total of 960 MAbs) were assayed in the primary screen. Each MAb pool (120 µL) was applied to one well of the Bio-Dot apparatus and allowed to pass through the membrane by gravity flow. The membrane was processed according to standard Western blotting techniques using anti-mouse HRP secondary antibody (1:2000 dilution in TBST; Amersham) and enhanced chemiluminescence detection (ECL, Amersham). To identify the anti-NIAM MAbs within the positive pools from the first screen, a second round of screening was performed on the individual MAb supernatants (30 µL) using the same Bio-Dot Western blotting approach. Cell colonies corresponding to each positive supernatant (sometimes each well had two or three colonies) were then expanded and retested in a final round of screening. MAb specificity to NIAM was confirmed by examining their reactivity to purified BSA and GST proteins, which were loaded onto the Bio-Dot filtration unit in an identical manner as the hNIAM polypeptide.

Cell lines and culture conditions

Several human pancreatic adenocarcinoma cell lines were used and maintained as follows: Panc-1 cells in Dulbecco's Modified Eagles' Medium (DMEM) containing 10% fetal bovine serum (FBS), 4 mM glutamine, and 100 µg/mL of penicillin and streptomycin; BxPC-3 cells in RPMI 1640 with 10% FBS; MIA PaCa-2 cells in DMEM supplemented with 10% heat-inactivated FBS and 2.5% horse serum. H6C7 cells, a non-transformed human pancreatic cell line, were maintained in Keratinocyte-SFM media supplemented with epidermal growth factor (EGF), BPE, and 2 mM glutamine. The entire pancreatic cell panel was kindly provided by Joseph Cullen (University of Iowa). Human U20S osteosarcoma cells and mouse NIH 3T3 fibroblasts were cultured in DMEM containing 10% FBS and 2 mM glutamine plus antibiotics. U20S cells expressing empty vector control (pCDF1-EF1-puro) or human NIAM (pCDF1-HA.hNIAM-EF1-puro) were generated by lentiviral infection and 2 day selection for puromycin-resistant cells (2 µg/mL). NIH 3T3 cells expressing empty pMSCV-IRES-GFP vector or pMSCV-mNIAM-IRES-GFP were generated by calcium phosphate transfection and selection of successfully transfected GFP-positive cells 2 days later by fluorescence activated cell sorting, as previously described.⁽¹⁴⁾ Stable polyclonal populations of H6c7 expressing NIAM knockdown (shNIAM) or point mutant control (shCON) short hairpin constructs were generated by puromycin selection (1 µg/mL for 2 days) following infec-

tion with pSUPER-retro-puro based retroviruses, as previously described.⁽¹³⁾

Western blot analyses

Frozen cell pellets were lysed on ice in NP-40 buffer (50 mM Tris [pH7.5], 120 mM NaCl, 1 mM EDTA, 0.5% NP-40) supplemented with 1 μ M NaF, 1 μ M leupeptin, and PMSF (phenylmethylsulfonyl fluoride). Lysates were sonicated (5 s pulse), incubated on ice for 30 min, and clarified by centrifugation at 14,000 rpm for 10 min at 4°C. An equivalent amount of protein from each sample was separated by SDS-PAGE on a 10% polyacrylamide gel and transferred to PVDF membrane (Millipore). Membranes were blocked with 5% nonfat dry milk in TBST (150 mM NaCl, 100 mM Tris-HCl [pH 8.0], 0.1% Tween-20) and incubated overnight at 4°C with each MAb supernatant (diluted at 1:2, 1:5, 1:10, or 1:20 in block solution). Membranes were probed with anti-mouse-HRP secondary antibody (1:2000 dilution, Amersham) and proteins visualized by ECL detection.

In vitro immunoprecipitation assay

Radiolabeled mNIAM and hNIAM proteins were generated by coupled *in vitro* transcription and translation (TNT kit, Promega, Madison, WI) using ³⁵S-TransLabel (ICN). Labeled proteins were then immunoprecipitated by overnight incubation at 4°C with each MAb supernatant (100 μ L) plus protein G-Sepharose (Santa Cruz Biotechnology, Santa Cruz, CA). The polyclonal antibody (1 μ g/mL) to the NIAM C-terminus was included as a positive control for immunoprecipitation. Samples were washed four times with NP-40 buffer at 4°C and immunoprecipitated NIAM protein detected by autoradiography following SDS-PAGE and transfer to a PVDF membrane.

Immunofluorescence

U2OS cells expressing vector control or hNIAM, as well as a panel of human pancreatic cell lines (H6C7, Panc-1, Mia-Paca-2, BxPC-3) expressing endogenous NIAM, were seeded at 3×10^4 cells per well onto eight-well poly-L-lysine coated chamber slides (Becton Dickinson, Franklin Lakes, NJ). The

next day, cells were fixed in either methanol-acetone (1:1) for 10 min at -20°C or 4% paraformaldehyde for 10 min at room temperature. Paraformaldehyde-fixed cells were then permeabilized with 0.1% Triton X-100 for 10 min at room temperature. Fixed cells were washed in PBS and stained with each hNIAM MAb at different dilutions (neat, 1:2, 1:5, or 1:20) followed by FITC-conjugated anti-mouse IgG (1:200 dilution, Amersham). The MAb VIII-E101 at a 1:5 dilution was optimal for detection of endogenous hNIAM. Nuclei were visualized with 4',6'-diamidino-2-phenylindole (DAPI) at 1 μ g/mL in ddH₂O for 1 min, and staining was analyzed by confocal microscopy (Zeiss) using 0.5 μ m optical slices.

Immunohistochemistry

All immunoperoxidase studies were done using the Dako-Cytomation Envision+ System-horse radish peroxidase (HRP) method with 3,3'-diaminobenzidine (DAB) as the chromogen (DakoCytomation, Carpinteria, CA). All rinses were performed using Dako wash buffer (Tris-buffered saline solution containing 0.05% Tween-20 [pH 7.6]), and antibody dilutions were performed using Dako antibody diluent buffer (0.05 mol/L Tris-HCL [pH 7.2-7.6], 1% BSA).

H6c7 pancreatic cell pellets were fixed in 10% neutral buffered formalin and paraffin embedded. Paraffin sections were cut at 4 μ m, applied to silanated slides (Fisher Scientific, Pittsburgh, PA) and air dried overnight at room temperature. The dried sections were oven baked at 60°C for 30 min and subsequently deparaffinized in xylenes, rehydrated in graded alcohols, and rinsed in distilled water. Antigen unmasking (retrieval) was performed via microwave processing in citrate buffer (pH 6.0), for two sequential heating cycles of 4 and 3 min. Slides were cooled at room temperature for 20 min prior to application of 3% hydrogen peroxide for quenching of endogenous peroxidase activity. Sections were incubated with NIAM MAb primary antisera at a dilution of 1:10, incubated overnight at 4°C, rinsed, covered with Envision+ System Labeled polymer HRP anti-mouse secondary antisera for 30 min, and then rinsed. Chromogenic visualization was achieved by incubating sections for 5 min with Dako Liquid DAB+ Substrate-Chromogen Solution, and slides were then rinsed and counterstained for 3 min with

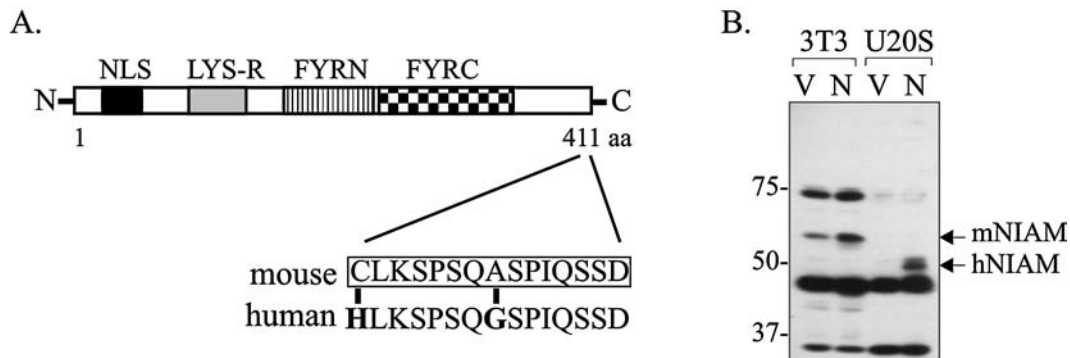


FIG. 1. Inability of the NIAM polyclonal antibody (pAb) to recognize endogenous human NIAM (hNIAM). (A) Schematic of the NIAM protein. A comparison of C-terminal residues in human and mouse NIAM is shown, with unique residues in hNIAM highlighted in bold. The pAb to NIAM was generated using the mouse NIAM (mNIAM) peptide (boxed). (B) Western blot using the NIAM pAb and lysates from mouse NIH 3T3 and human U2OS cells expressing empty vector (V) or exogenous mouse or human NIAM (N), respectively.

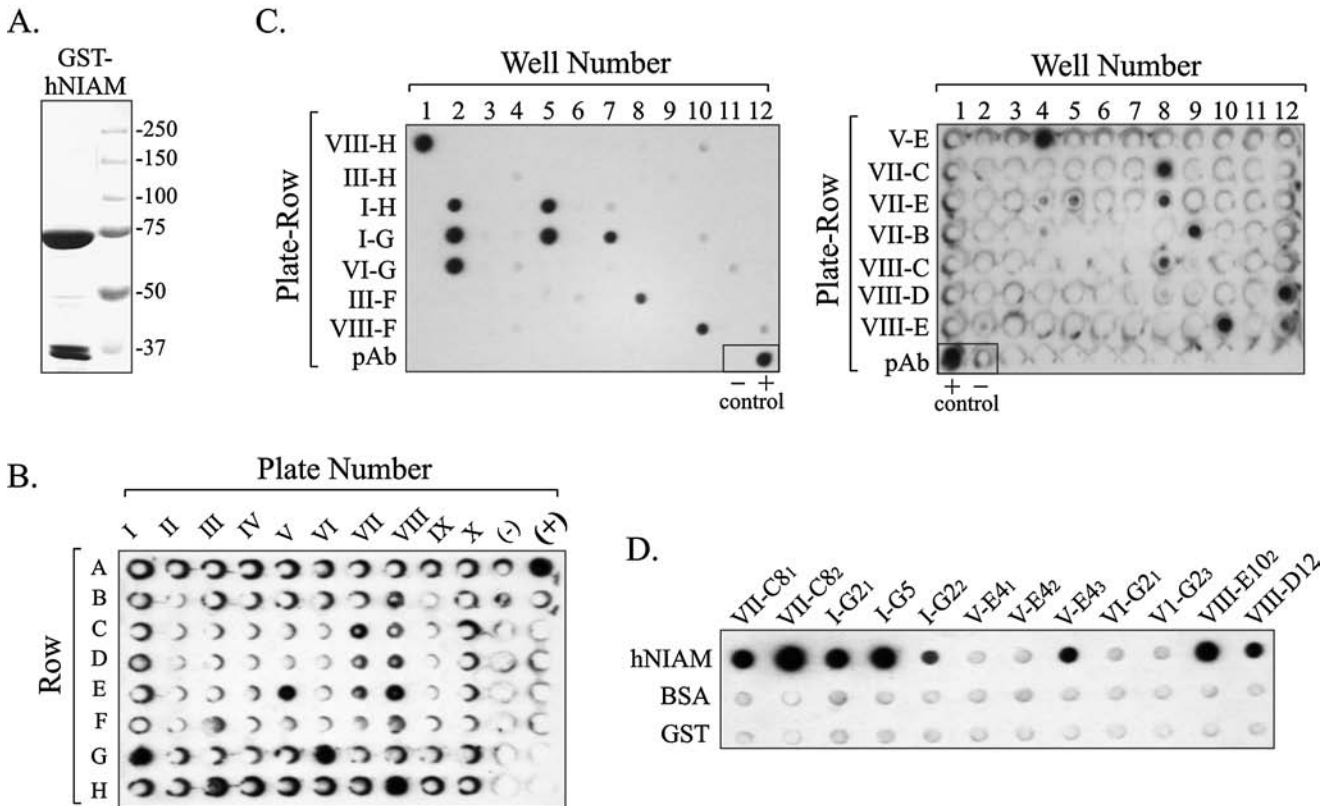


FIG. 2. NIAM MAb screening. (A) Coomassie blue-stained gel of purified GST-hNIAM protein. Sizes of the protein standards are indicated. (B) Western blot from the first round of MAb screening using GST-hNIAM as antigen on dot blots and pooled hybridoma supernatants (12 different supernatants from one row of a 96-well plate). The plate number and row from which each pool was obtained are denoted, as are the negative (-) and positive (+) controls. (C) Western blot results from the second round of MAb screening in which individual MAb supernatants were tested, as indicated. (D) Third and final round of MAb screening that examined the specificity of each supernatant for hNIAM as opposed to purified BSA or GST.

Harris formula hematoxylin (Surgipath Medical Industries, Richmond, IL). Negative control slides were with non-immune mouse immunoglobulin G (MIgG) at a dilution of 1:1000 in lieu of the NIAM MAb.

Results

Inability of polyclonal antibodies to recognize endogenous human NIAM

The human and mouse NIAM cDNAs encode polypeptides of ~50 kDa and 55–60 kDa, respectively.⁽¹³⁾ Both predicted proteins contain nuclear/nucleolar localization sequences (NLS), a lysine rich region (LYS-R), and two poorly understood domains abundant in phenylalanine, tyrosine, and arginine (FYRN and FYRC) (Fig. 1A). We had previously generated rabbit polyclonal antibodies (pAb) to the extreme C-terminus of mouse NIAM, a region in which 13 of the 15 residues are identical to the human protein (Fig. 1A). Immunoblotting showed the pAb effectively recognizes endogenous and overexpressed mNIAM in NIH 3T3 cells, as well as ectopically expressed hNIAM in human U2OS cells (Fig. 1B). Conversely, the pAb was unable to detect endogenous hNIAM cells (Fig. 1B) or any other human cells tested.⁽¹³⁾ Based on these data, it was not possible to determine if the pAb sensitivity was too low to detect low levels of endogenous protein or if hNIAM was not expressed in the cells examined.

Screening for hNIAM monoclonal antibodies by immunoblotting

To define the role of hNIAM in carcinogenesis, it is crucial to be able to detect the endogenous protein in human cell and tissues. Therefore, we sought to develop monoclonal antibodies (MAb) to hNIAM. Recombinant hNIAM was expressed as a glutathione S-transferase (GST) fusion pro-

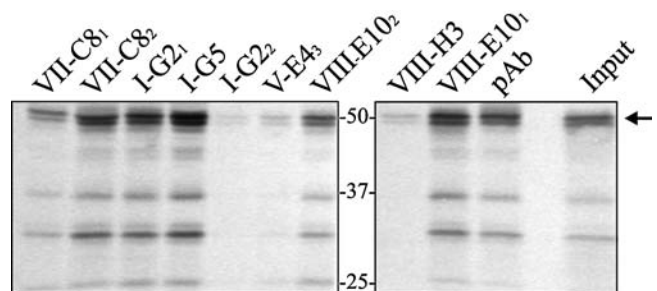


FIG. 3. Immunoprecipitation (IP) assay comparing the ability of different MABs to recognize *in vitro* translated radiolabeled hNIAM. The full-length hNIAM IVT product is indicated (arrow). As a positive control, the IVT product was immunoprecipitated by the NIAM pAb. Input represents 25% of the IVT added to each IP reaction.

TABLE 1. COMPARISON OF NIAM MAb ACTIVITIES IN WESTERN BLOT, IP, AND IF ANALYSIS

NIAM MAb	Western detection hNIAM vs. mNIAM	IP recognition hNIAM vs. mNIAM	IF hNIAM ^c
I-G2 ₁	Yes, Yes ^a	Yes, ^a No	Yes
I-G5	Yes, ^b Yes ^a	Yes, Yes	Yes
V-E4 ₃	Yes, ^b No	Yes, ^a No	NT
VII-C8 ₁	Yes, ^b Yes ^a	Yes, No	Yes
VII-C8 ₂	Yes, ^b Yes ^a	Yes, No	Yes
VIII-B9 ₁	No, No	Yes, No	NT
VIII-D12	Yes, ^b No	No, No	NT
VIII-E10 ₁	Yes, No	Yes, No	Yes
VIII-E10 ₂	Yes, No	Yes, No	No

^aWeak detection.

^bDetection of exogenous protein only.

^cDetection of endogenous hNIAM in H6c7 epithelial cells.

tein in bacteria, recovered on glutathione Sepharose, and purified by gel extraction following SDS-PAGE (Fig. 2A). GST-hNIAM was then used as antigen to immunize mice and generate hybridomas. In the initial screen to identify MABs that recognize hNIAM, the GST-hNIAM protein was applied to membranes in a dot-blot apparatus and Western blotting was performed using pools of hybridoma supernatants (Fig. 2B). The rabbit pAb to NIAM or sera from the immunized mouse were used as positive controls whereas no primary antibody served as the negative control. Of 80 MAB pools tested (each containing 12 different supernatants from a row of a 96-well plate), 14 (e.g., VIII-E or I-G) were chosen for a second round of screening of individual well supernatants by the same method (Fig. 2C). Hybridoma clones corresponding to each positive supernatant were then expanded and retested for specificity to hNIAM (Fig. 2D). In some cases, multiple colonies were present in each well and they were tested individually (e.g., VII-C8₁ and VII-C8₂). Other clones, such as VI-G2₁ and VI-G2₃, lost reactivity to hNIAM over time (Fig. 2C and D). None of the MABs recognized GST or BSA (Fig. 2D). Thus, these screens were successful in identifying several MABs that specifically detect hNIAM by immunoblotting.

Identification of MABs that immunoprecipitate hNIAM *in vitro*

The ability of each MAB to effectively immunoprecipitate (IP) the native hNIAM protein was assayed using radiolabeled *in vitro* translated (IVT) hNIAM (Fig. 3). Immune complexes were captured on Protein G-agarose, separated by SDS-PAGE, and the presence of immunoprecipitated hNIAM detected by autoradiography. The most effective MABs able to IP hNIAM were I-G5, VIII-E10₁, I-G2₁, and VII-C8₂ (Fig. 3). By comparison, only I-G5 recognized a mNIAM IVT product by IP (data not shown). Other MABs either failed to effectively IP hNIAM (I-G2₂, V-E4₃, and VIII-H3) or did so at an intermediate level (VII-C8₁ and VIII-E10₂). These results, as well as data from subsequent assays described below, are summarized in Table 1.

Differential ability of MABs to detect endogenous hNIAM

Western blotting was then used to assess the specificity of each MAB for hNIAM, as opposed to mNIAM, and to test their ability to recognize endogenous hNIAM from mammalian cell lysates (Fig. 4). Whole cell lysates from human U2OS cells expressing empty vector or exogenous hNIAM,

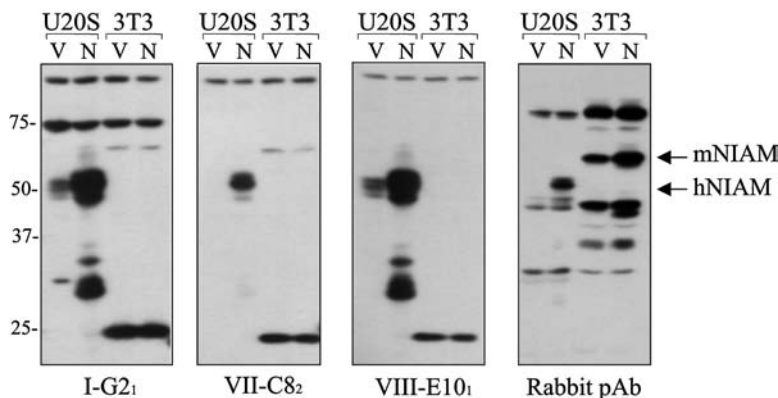


FIG. 4. Identification of MABs capable of detecting endogenous hNIAM by immunoblotting. Representative Western blots are shown that compare the reactivity of the NIAM pAb and MABs with either mNIAM or hNIAM. Human U2OS and mouse 3T3 cell lysates containing empty vector (V) or exogenous human or mouse NIAM (N) were examined. Positions of the protein standards are indicated on the left, while mNIAM and hNIAM are designated by arrows on the right.

as well as mouse NIH 3T3 cells expressing vector control or exogenous mNIAM, were subjected to Western blotting with each MAb supernatant or the pAb. A representative set of blots is shown in Figure 4 while Table 1 lists the results for all the MAbs tested. While the pAb recognized endogenous mNIAM in addition to overexpressed mNIAM and hNIAM, the MAbs were highly specific for the human form of the protein and only faintly recognized mNIAM (I-G2₁ and VII-C8₂), or not at all (VIII-E10₁). Most importantly, a few MAbs such as I-G2₁ and VIII-E10₁ effectively detected endogenous hNIAM in vector-transfected U2OS cells.

MAb VIII-E10₁ was subsequently used to assess the levels of endogenous hNIAM expression by immunoblotting in a small panel of human pancreatic cancer cell lines (Fig. 5A). These lines were analyzed based on our previous finding that hNIAM mRNA is downregulated in the tumor-derived cells (Mia PaCa-2, Panc-1, and BxPC-3) compared to non-transformed pancreatic epithelial cells (H6c7).⁽¹³⁾ Based on those results, we expected the cancer cell lines to express the least amount of NIAM compared to H6c7 cells. Interestingly, while H6c7 cells displayed the lowest level of NIAM by im-

munoblotting (Fig. 5A), they yielded the strongest staining intensity when hNIAM localization was assayed by immunofluorescence (IF) and confocal microscopy (Fig. 5B; note that the U2OS and Panc1 cells had relatively weak signal intensities for hNIAM that cells were compensated for by different microscope settings and are consequently not reflected in the images shown). Other NIAM MAbs were then tested for their ability to detect endogenous NIAM by IF in H6c7 cells. Results showed identical staining patterns of similar intensity for all MAbs assayed with the exception of VIII-E10₂, which gave no signal by IF (Table 1).

Differential detection of hNIAM by blotting and IF using the VIII-E10₁ MAb was also seen in analyses of Mia PaCa-2 and BxPC-3 cells. Both cells expressed relatively high levels of endogenous hNIAM by immunoblotting (Fig. 5A) but only BxPC-3 showed staining for the protein by IF (data not shown). Different fixation conditions (1:1 methanol-acetone versus 4% para-formaldehyde) were tested, but only the latter worked effectively. Perhaps most striking was the observation that hNIAM resides in the nucleus in U2OS and Panc1 cells, as expected from previous studies of NIAM,⁽¹³⁾ but ap-

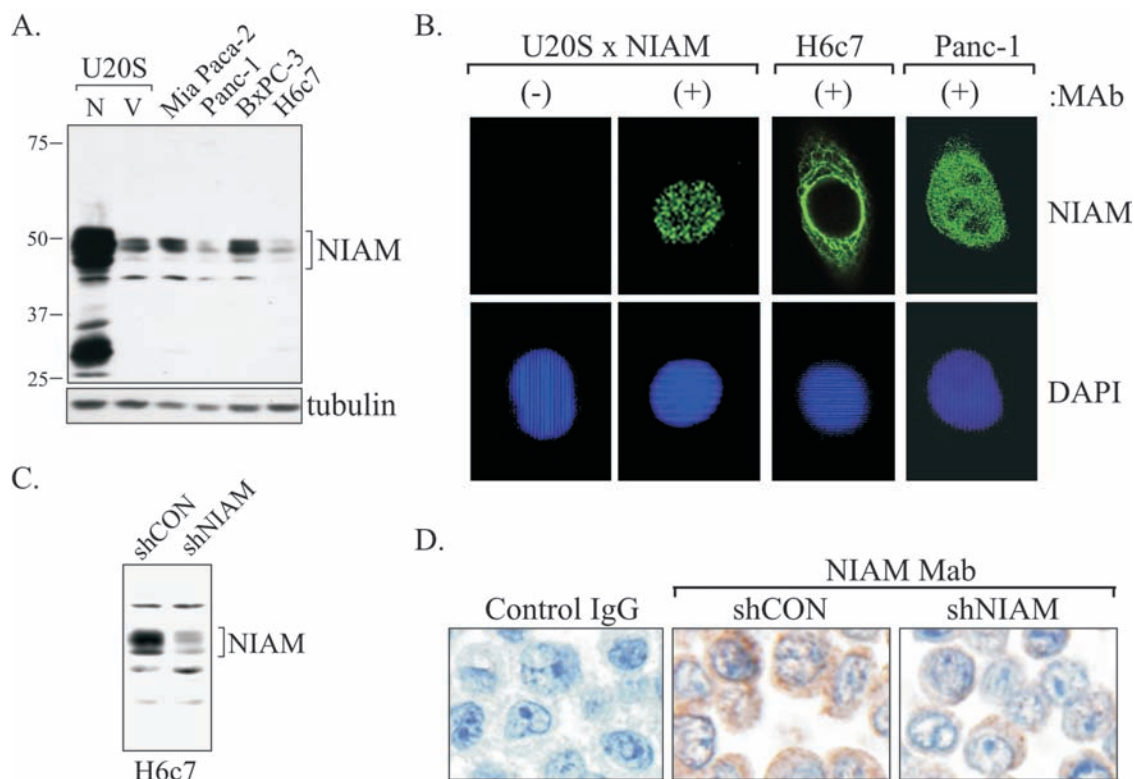


FIG. 5. Detection of endogenous hNIAM by IF and IHC using MAb VIII-E101. (A) Western blot showing endogenous hNIAM expression levels in Mia PaCa-2, Panc-1, BxPC-3, and H6c7 pancreatic cells as well as U2OS cells expressing vector (V) or exogenous hNIAM (N). Tubulin served as a loading control. (B) IF analyses of U2OS expressing exogenous hNIAM and parental Panc-1 and H6c7 cells expressing endogenous hNIAM. Confocal images (0.5 μ m slices) were taken from samples stained with (+) or without (-) primary VIII-E10₁ MAb. Different microscopic settings were used to capture images, for which the signal intensity was markedly weaker in U2OS and Panc-1 cells compared to H6c7 cells. DAPI staining was used as a marker for nuclei. (C) Western blot showing reduced hNIAM expression in H6c7 cells with NIAM knockdown (shNIAM) compared to controls (shCON). (D) IHC staining of formalin-fixed paraffin-embedded H6c7-shCON and H6c7-shNIAM cells. The brown stain indicative of hNIAM expression in the cytoplasm (middle panel) was not observed in controls stained with mouse IgG (left panel) and was greatly reduced in shNIAM knockdown cells (right panel).

pears perinuclear and cytoplasmic in H6c7 cells (Fig. 5B). Notably, cytoplasmic staining is also evident in the Panc1 cells (Fig. 5B), and identical staining patterns were observed using other NIAM MABs (data not shown and Table 1).

To test the specificity of the NIAM staining in H6c7 cells, stable polyclonal populations with NIAM knockdown (shNIAM) or point mutant control constructs (shCON) were generated. Effective and selective NIAM knockdown was obtained with approximately 70% reduction in protein expression levels (Fig. 5C). Cells were then fixed in formalin, embedded in paraffin, and treated with either mouse IgG or NIAM MAB VIII-E101 to assess NIAM expression and localization by immunohistochemistry (IHC). In keeping with the localization pattern of hNIAM by IF, IHC staining of H6c7-shCON cells yielded a strong cytoplasmic signal compared to those incubated with control mouse IgG (Fig. 5D). Moreover, detection of NIAM was greatly reduced in H6c7-shNIAM cells in accordance with the decreased expression by immunoblotting. These results demonstrate the specificity and potential utility of MAB VIII-E101 for the detection of endogenous hNIAM in formalin-fixed paraffin-embedded human tissue samples.

Discussion

This study describes the successful development of multiple MABs that selectively recognize the human NIAM protein. All MABs were either highly specific for hNIAM or only detected the mouse form of the protein weakly. Importantly, several MABs were identified that effectively detected endogenous hNIAM by immunoblotting and IF, and one of those antibodies (VIII-E101) was found to work well in IHC assays. At present, the optimal MABs identified from the screen for analyses of endogenous hNIAM by various assays (Western, IF, and IHC) include VIII-E101, I-G21, and I-G5.

NIAM was named, in part, because it was originally found to be a nuclear protein in both mouse and human cells.⁽¹³⁾ However, IF and IHC analyses with any of the MABs tested revealed that hNIAM is not always localized to the nucleus in all cells since it is cytoplasmic in H6c7 cells and both cytoplasmic and nuclear in Panc1 cells. The observation that endogenous hNIAM is nuclear in Panc1 pancreatic cancer cells, similar to exogenous hNIAM in U2OS cells, suggests that nuclear localization is not an artifact of overexpression. We then considered the possibility that NIAM subcellular localization differs depending on whether cells are non-transformed (H6c7) or derived from tumors (U2OS, Panc1). However, analyses of BxPC-3 cancer cells revealed a similar pattern of localization as that seen in H6c7 cells (data not shown). More studies are clearly warranted to determine the mechanism and physiological significance of the differential subcellular localization of hNIAM in various cells.

Interestingly, the VIII-E10 MAB displayed a differential ability to detect endogenous hNIAM in the pancreatic cell lines depending on the cell and type of approach (Western versus IF). Whereas high levels of hNIAM protein were observed in the Mia PaCa-2 cells by Western blot, no protein was detected in those cells by IF. An opposite pattern was seen in H6c7 cells in which hNIAM was poorly detected by Western blot but robustly stained by IF. Western blots enable detection of denatured proteins from whole cell lysates; thus, if one assumes equivalent extraction of hNIAM from

the different cells, it should provide an accurate comparison of total hNIAM expression levels. By comparison, proteins are fixed in their native state during IF such that particular epitopes of MAB recognition could be masked by hNIAM tertiary structure or its association with other molecules. Therefore, our results suggest hNIAM conformation and/or molecular interactions differ in the various cells examined. Whether or not this correlates with differential activity of hNIAM in those cells remains to be determined.

Previous analyses of NIAM showed that its loss accelerates chromosomal instability in cells lacking p53 and ARF.⁽¹³⁾ Moreover, microarray data show that NIAM mRNA is downregulated in a large variety of human cancers.⁽¹³⁾ Given that NIAM has antiproliferative activity that intersects with ARF-Mdm2-p53 signaling, such findings strongly support the idea that NIAM is a new tumor suppressor. The identification of MABs in this study that effectively detect endogenous human NIAM by Western blot, IF, IP, and IHC now enables us to directly test that hypothesis and possibly establish new paradigms of carcinogenesis.

Acknowledgments

This work was supported by grant # CA90367 from the NIH (DEQ). The study could not have been completed without the invaluable contributions of Chuck Lovig at the University of Iowa Hybridoma Core Facility, and Christine Hochstedler and Ed Solin at the University of Iowa Core Pathology Research Laboratory.

References

- Hanahan D, and Weinberg RA: The hallmarks of cancer. *Cell* 2000;100:57-70.
- Vogelstein B, Lane D, and Levine AJ: Surfing the p53 network. *Nature* 2000;408:307-310.
- Sherr CJ, and McCormick F: The RB and p53 pathways in cancer. *Cancer Cell* 2002;2:103-112.
- Hainaut P, Soussi T, Shomer B, Hollstein M, Greenblatt M, Hovig E, Harris CC, and Montesano R: Database of p53 gene somatic mutations in human tumors and cell lines: updated compilation and future prospects. *Nucl Acids Res* 1997; 25:151-157.
- Quelle DE, Zindy F, Ashmun RA, and Sherr CJ: Alternative reading frames of the INK4a tumor suppressor gene encode two unrelated proteins capable of inducing cell cycle arrest. *Cell* 1995;83:993-1000.
- Ruas M, and Peters G: The p16INK4a/CDKN2A tumor suppressor and its relatives. *Biochim Biophys Acta* 1998;1378: F115-77.
- Lowe SW, and Sherr CJ: Tumor suppression by Ink4a-Arf: progress and puzzles. *Curr Op Genet Dev* 2003;13:77-83.
- Sherr CJ: Divorcing ARF and p53: an unsettled case. *Nat Rev Cancer* 2006;6:663-673.
- Iwakuma T, and Lozano G: MDM2, an introduction. *Mol Cancer Res* 2003;1:993-1000.
- Christophorou MA, Ringshausen I, Finch AJ, Swigart LB, and Evan GI: The pathological response to DNA damage does not contribute to p53-mediated tumour suppression. *Nature* 2006;443:214-217.
- Ha L, Ichikawa T, Anver M, Dickins R, Lowe S, Sharpless NE, Krimpenfort P, DePinho RA, Bennett DC, Sviderskaya EV, and Merlino G: ARF functions as a melanoma tumor

- suppressor by inducing p53-independent senescence. *Proc Natl Acad Sci USA* 2007;104:10968–10973.
12. Tompkins V, Hagen J, Zediak VP, and Quelle DE: Identification of novel ARF binding proteins by two-hybrid screening. *Cell Cycle* 2006;5:641–646.
 13. Tompkins VS, Hagen J, Frazier AA, Lushnikova T, Fitzgerald MP, di Tommaso A, Ladeveze V, Domann FE, Eischen CM, and Quelle DE: A novel nuclear interactor of ARF and MDM2 (NIAM) that maintains chromosomal stability. *J Biol Chem* 2007;282:1322–1333.
 14. Zhao L, Samuels T, Winckler S, Korgaonkar C, Tompkins V, Horne MC, and Quelle DE: Cyclin G1 has growth inhibitory activity linked to the ARF-Mdm2-p53 and pRb tumor suppressor pathways. *Mol Cancer Res* 2003;1:195–206.

Address reprint requests to:

Dawn E. Quelle
Department of Pharmacology
The University of Iowa
College of Medicine
2-370 BSB
51 Newton Rd.
Iowa City, Iowa

E-mail: dawn-quelle@uiowa.edu

Received: August 29, 2007

Accepted after revision: February 12, 2008